



Association between nonlinear dynamic characteristics of ground motions and resonance in soil

Hanif Rahmani¹ · Farhang Rahmani²

Received: 23 October 2021 / Accepted: 26 February 2022 / Published online: 4 April 2022
© Saudi Society for Geosciences 2022

Abstract

Resonance in the soil increases the earthquake force applied to buildings and can lead to serious damage to structures. Due to the importance of the resonance in soil for structural design, this study attempted to clarify the effect of earthquake signals' nonlinear dynamic properties on soil resonance. This objective was accomplished by generating an artificial soil profile using DEEPSOIL software, which contained 16 layers and had a shear wave velocity (m/s) of 987.025696004126. Ten common strong ground motion records were applied to a soil profile. First, resonance in the soil was investigated in response to the application of ten ground motions. Subsequently, the nonlinear dynamic properties of the earthquake acceleration time series were investigated, and the relationship between the earthquake signals' nonlinear dynamic properties and the resonance in the soil was evaluated. The results indicated that ground motions with symmetrical or right tail multifractal singularity spectrum curves triggered resonance probability in soil. Ground motions with a mono-scale structure raised the likelihood of resonance in soil more than motions with a multifractal structure. The soil resonance probability was augmented by long memory and the anti-correlated behavior of the ground motions. The findings suggest that in the case of structural design, when assessing the risk of resonance in the soil, the only ground motions considered should be those having at least one condition of the mono-scale structure or multifractal structure with symmetrical- or right-tail singularity spectrum.

Keywords Newmark β method · Time domain analysis · Multifractal detrended fluctuation analysis (MF-DFA) · Generalized holder exponent · Correlation · Soil failure

Introduction

Earthquake waves are transformed as they diverge from the epicenter and go through the alluvial layers. Factors related to the distance of points from the epicenter are known as “path impacts,” and factors associated with alluvial layers located on the bedrock are known as “site effects.” Site effects manifest in the form of the intensification of earthquake waves and alterations in seismic waves' characteristics such as their amplitude, frequency, and the duration of strong movements. Today, earthquakes are one of the most

devastating natural disasters leading to the destruction of man-made structures. Several destructive earthquakes in recent decades, including those in Mexico City (1985), North Ridge (1994), and Turkey (1999), as well as severe earthquakes in Iran, such as that which affected Bam (2003), have clearly revealed that the geological conditions and surface topography play influential roles in the extent of vibrations. As a case in point, consider the Mexico City earthquake. On September 19, 1985, an earthquake with an 8.1 magnitude on the Richter scale struck Mexico, brought about moderate damage to its epicenter (Pacific coast); however, it produced severe damage 350 km away in Mexico City. Another case is the earthquake that occurred on November 13, 2017, at the Sare Pole Zahab in Kermanshah province, Iran. Expert groups who were sent to the area to assess various aspects of the earthquake detected that the damage distribution was not uniform; there were significant differences in distinct parts of the city, even between comparable types of structures. There were two types of structural damage. In the northern sections of the city's main boulevard,

Responsible Editor: Longjun Dong

✉ Farhang Rahmani
farhang.rahmani@miau.ac.ir

¹ Department of Civil Engineering, Estahban Branch Islamic Azad University, Estahban, Iran

² Department of Civil Engineering, Marvdasht Branch Islamic Azad University, Marvdasht, Iran

the damage was insignificant even though most of the other areas were severely damaged.

In 1996, Kaiser et al. (1996) proposed that two parameters, peak ground velocity (PGV) and peak ground acceleration (PGA), could be used to estimate the dynamic vibration load. Ground motions can be quantified by these two parameters. During an earthquake, the accumulated energy in the focal area is released in the form of seismic waves. The focal mechanism is an important feature of the seismic source that influences the propagation of seismic waves. In other words, the ground motions generated by earthquakes are closely related to the focal mechanism. Even if the distance to the source is the same in different directions, the dynamic load can vary significantly (Ma et al. 2018, 2019).

Douglas et al. (2007) conducted research examining focal mechanism effects on the earthquake ground motions. They reported a considerable influence of the focal mechanism on ground motion produced by earthquakes. Mining studies also indicated the importance of focal mechanisms (Ma et al. 2019). According to extant theories, the vibrations produced by the explosion are reduced in all directions away from the source of the explosion. However, Ma et al.'s (2019) results showed that the ground vibrations did not decrease as they moved away from the source of the explosion; this phenomenon was due to the focal mechanism parameter.

Additionally, ground motions are distance-related and azimuth-related in spatial distribution. Alluviums with diverse structures show different responses due to the arrival of earthquake waves. Researchers have also revealed that responses to a particular earthquake vary from station to station due to the characteristics of various sites (Pavel et al. 2020; Ottonelli et al. 2021; Alam et al. 2021). Other researchers have reported similar results who used a similar approach to the present study, including Zheng et al. (2021) and Alimohammadi et al. (2020, 2019a, b), Alimohammadi and Yaghin (2019). The geological properties of the site are a fundamental factor influencing seismic responses (Diaz-Fanas et al. 2020). For example, when the environment structure has horizontal layers, only volumetric waves moving up and down in the surface layers are trapped, whereas when the environment structure is two- or three-dimensional (lateral heterogeneity), the surface waves created by this inconsistency are also trapped.

Soil stratification close to the surface can significantly intensify or weaken seismic forces (Garcia-Suarez and Asimaki 2020). Resonance in the soil is of great significance for structural design, as structures vulnerable to resonance can be destroyed easily (Mase et al. 2021). So far, numerous studies have been conducted on soil resonance from various perspectives (Gosar et al. 2010; Kaurkin et al. 2021; Guangyin et al. 2021; Trevisani et al. 2021; Xie et al. 2020; Moschetti and Hatzell 2021; Sgattoni and Castellaro 2020; Gallipoli et al. 2020). The term resonance

relates to the increase in amplitude when the frequency of an applied alternating force to a system is equal to or close to the system's natural frequency. By applying an oscillating force to a dynamic system resonant frequency, the system oscillates at a higher amplitude than in cases where an equal force is applied to other non-resonant frequencies (Halliday et al. 2005).

Studies conducted by the Roads, Housing and Urban Development Research Center to present the structure design regulations against earthquakes in Iran (Regulations 2800 (2014)) suggest that replacing the hard soil layer close to the earth's surface with soft soil (sand to gravel) intensified the earthquake motion on the ground surface (thus intensifying the ground motion response curve). Moreover, by doubling the soil layer thickness (the soil close to the ground surface was assumed to be coarse-grained), the movement of the ground surface was weakened. Thus, the possibility of soil resonance was significantly reduced as a direct consequence of the increase in the thickness of the damper soil layers (sand and gravel).

Additionally, a reduction in the arrival acceleration into the soil intensified the ground response. This effect can be explained by the fact that moderate earthquakes produce more soil resonance than strong earthquakes due to damping. Small earthquakes produce minute strains, and in tiny strains, damping is slightly activated. Conversely, large earthquakes generate considerable strains, providing an enormous amount of damping, thereby reducing the severity of ground movements.

The importance of studying the phenomenon of resonance in the soil, as well as the factors affecting ground motions and the phenomenon of resonance in soil, was mentioned above. Due to the importance of the resonance in the soil for structural design, this phenomenon should be studied from different perspectives.

The present study is of relevance because it examines factors affecting resonance in soil from different perspectives. However, the effect of dynamic properties and repetitive patterns in earthquake signals on resonance in soil has not been studied, which is addressed in this study. This study contributes to the understanding of the effect of dynamic properties and repetitive patterns in earthquake acceleration time series on resonance in soil. It provides the impetus for future research on the effect of earthquake signals on the resonance phenomenon in soil. This study demonstrates whether, in addition to properties of soil, focal mechanisms, distance, and nonlinear dynamic properties of ground motions, among other factors, affect the resonance in soil. It also suggests which ground motions should be considered in the case of structural design to examine resonance in the soil. This research is beneficial to structural design and soil engineers and researchers who study the effect of earthquake signals on soil behavior.

The main objective of the present study is achieved by generating a soil column with sixteen horizontal layers. Subsequently, ten well-known earthquake accelerations (motions) were applied to the soil column to study soil resonance and soil failure. Ultimately, the multifractal detrended fluctuation analysis (MF-DFA) technique was employed to estimate the nonlinear dynamic properties of motions, and subsequently, the association between the earthquake signal's nonlinear dynamic properties and soil resonance was investigated.

In the next section, the soil column and earthquake details used for analysis will be provided. In the “**Results and discussion**” section, the results will be presented and discussed. Finally, the “**Conclusion**” section will provide a summary and conclusions.

Materials and methods

In order to investigate the effect of earthquakes on generated soil profile, ten well-known motions (earthquakes) were considered, and acceleration data were collected from PEER Ground Motion Database (<https://ngawest2.berkeley.edu/>). Details concerning the ten utilized motions (earthquakes) are sorted in Table 1.

Earthquakes that occurred between 1940 and 1995 and ranged in magnitude from 6.8 to 7.3 Mw were examined in this study. The lowest (5 km) and highest (19 km) depths at which the earthquakes occurred were the earthquakes of SPITAK and LOMA, respectively. The ten investigated earthquakes occurred in different countries. The location of the Kobe earthquake is shown in Fig. 1. This earthquake was recorded in 1995 and had a depth of 17.6 km; approximately 6434 people lost their lives.

Generating soil profile and plotting shear strain percentage and 5% damped spectral acceleration

After collecting earthquake data, a soil profile was generated using DEEPSOIL software version 7. The soil profile was generated by employing the techniques of generalized quadratic/hyperbolic (GQ/H) model with shear strength control, proposed by Groholski et al. (2016), and non-masing unload-reload rules, proposed by Phillips and Hashash (2009). This soil model was selected because it requires few input data requirements (the curve fitting parameters θ_1 through θ_5 values and maximum stress τ_{max}), and DEEPSOIL software calculates the curve-fitting parameters of the generated soil profile.

The minimum thickness of the layers in the study soil profile was 1.9 m, and the total soil profile thickness was 30 m. The maximum frequency in the soil layers was 50 HZ, and the mean layer properties (including width, unit weight, and effective vertical stress) were 30 m, 20 KN/m³, and 152.85 KPA, respectively. The shear wave velocity varied according to the depth; specifically, it was 70 for the ground's surface and 700 for a depth of 30 m. The shear strength and soil type were 100 KPa and sand, respectively. The soil properties of each layer are provided in Table 2.

There are two general methods used to analyze soil response based on the ingress of an earthquake wave into the soil profile: the frequency-domain method and the time-domain method. The nonlinear time-domain method was employed to solve motion equations to estimate soil responses. This method was selected because it produces more reliable results than other methods.

Likewise, there are two available time integration methods used to solve motions equations: the Newmark β method (implicit) and the Heun Method (explicit). In the present study, the first method was adopted. Usually, to solve a second-order differential equation, one must first transform

Table 1 The details of the ten employed motions (earthquakes)

Motion name	Magnitude	Year	Type or mechanism	Epicenter	Fault	Depth
Borah Peak	6.88 Mw	1983	Normal	44.08°N 113.8°W	Lost River Fault	16 Km
Cape Mendocino	7.01 Mw	1992	Reverse	40.33°N 124.23°W	Mendocino Triple Junction	10.5 Km
El Alamo	6.8 Mw	1956	Strike Slip	-	-	-
Gazli, USSR	6.8 Mw	1976	Reverse	40.31°N 63.72°E	-	10 Km
Imperial Valley-2 (El Centro Array)	6.95 Mw	1940	right-lateral strike-slip	32°44'N 115°30'W	-	16 Km
Kobe	6.9 Mw	1995	Strike Slip	34.59°N 135.07°E	Nojima	17.6 Km
Loma Prieta	6.93 Mw	1989	Reverse Oblique	37.04°N 121.88°W	-	19 Km
Spitak, Armenia	6.77 Mw	1988	Reverse Oblique	40.987°N 44.185°E	-	5 Km
Taiwan Smart	7.3 Mw	1986	Reverse	Lat. 24 Lon. 121.8	-	15 Km
Trinidad	7.2 Mw	1980	Strike Slip	-	-	10 Km

Fig. 1 The location of the Kobe earthquake (marked with an asterisk) recorded in 1995



Table 2 Details concerning the generated soil layers through DEEPSOIL software version 7

Layer number	Thickness (m)	Unit weight (KN/m ³)	Shear wave velocity (m/s)	Effective vertical stress (KPa)	Shear strength (KPa)
1	1.9	20	987.025696004126	9.6805	100
2	1.6	20	987.025696004126	27.513	100
3	0.5	20	987.025696004126	38.2125	100
4	1	20	987.025696004126	45.855	100
5	2	20	987.025696004126	61.14	100
6	1	20	987.025696004126	76.425	100
7	1.7	20	987.025696004126	90.1815	100
8	2	20	987.025696004126	109.033	100
9	3	20	987.025696004126	134.508	100
10	3	20	987.025696004126	165.078	100
11	1.5	20	987.025696004126	188.0053	100
12	0.8	20	987.025696004126	199.724	100
13	2.5	20	987.025696004126	216.5375	100
14	3	20	987.025696004126	244.56	100
15	2.5	20	987.025696004126	272.5825	100
16	2	20	987.025696004126	295.51	100

that equation into two first-order differential equations. The advantage of the Newmark method (Newmark, 1959) is that it enables us to solve the second-order differential equation without the transformation (for further details, see Lindfield and Penny 2019).

DEEPSOIL software was utilized to solve the equations of the motion and extract shear strain percentage and 5% damped spectral acceleration graphs. According to the valid regulations (such as Regulations 2800 (2014)), when the shear strain percentage touches a value greater than 1%, the

soil is ruptured (soil failure phenomenon). The shear strain percentage curves were related to the investigation of the soil failure phenomenon in layers of the study soil profile. Depicting 5% damped spectral acceleration versus period graphs supports the study of the resonance in soil by examining the response spectra.

The phenomenon of resonance in soil occurs when the response spectra curve in a layer of soil exceeds the response spectra curve of the input motion into the soil profile. The significant duration of the ground motions was extracted

prior to the nonlinear dynamic properties’ estimation of ground motions. The significant duration is the time span (in seconds) between the occurrences of 5% and 95% of the total Arias Intensity. Arias Intensity can be used to represent the intensity of a motion as a function of acceleration (Eq. 1). The significant duration was computed using DEEPSOIL software. Ultimately, the nonlinear dynamic characteristics of the motions’ significant durations were estimated.

$$I_a(t) = \frac{\pi}{2g} \int_0^t [a(t)]^2 dt \tag{1}$$

Multifractal detrended fluctuation analysis (MF-DFA)

The application of detrended fluctuation analysis (DFA) is commonly adopted for the measurement of mono-fractal scaling characteristics and exploring long-range correlations in noisy, non-sub-basinary time series (Kantelhardt et al. 2002). Multifractal detrended fluctuation analysis (MF-DFA) technique can be used for multifractality assessment in the time series, and its accurate results for non-sub-basinary series (Adarsh et al. 2020; Miloş et al. 2020) prove the proper functionality of this tool for finding multifractal patterns in the hydrological time series. This technique also can be used for generalized Hurst exponent estimation. Accordingly, the MF-DFA technique was adopted to examine generalized Hurst exponent. The singularity spectrum $f(\alpha)$ can be employed for representing the multifractal patterns in the time series. The scaling exponent $\tau(q)$ and first-order Legendre transforms provide a basis for singularity spectrum evaluation (Eq. (2)), demonstrating the time series segment dimensions identified by α (see Eq. (3)). If $f(\alpha)$ is a single point, it can be concluded that the time series is mono-fractal (for further details, see (Rahmani and Fattahi 2021a)).

$$\tau(q) = q \times H(q) - 1 \tag{2}$$

$$\alpha = \frac{\partial \tau(q)}{\partial q}, f(\alpha) = \alpha q - \tau(q) \tag{3}$$

where α and q are the Hölder exponent (singularity index) and the local variations’ order weighting, respectively. $H(q)$ points to the generalized Hurst exponent and can be assessed by Eq. (4).

$$F_q(s) \propto s^{H(q)} \tag{4}$$

Equation 4 is known as the power-law association between variation segment $F_q(s)$ and time scale s . The $H(q)$ is valued by gradient of the fitted $F_q(s)$ and s (for further details concerning MF-DFA, see Mandelbrot 1989, Rahmani and Fattahi 2021b).

A narrow singularity spectrum depicts relative systematic fluctuations in the time series that occur over similar amplitudes over time; this is a sign for a mono-scaling structure. A wide singularity spectrum illustrates more periodic fluctuations in the time series that occur over a greater range of amplitudes in different time lengths, resembling the multifractal processes. The range of the singularity spectrum represents the dynamics of the system (Zhang et al. 2019; Munro et al. 2018).

The large fluctuations in a signal hold small singularity exponent α and are located in the left tail of the spectrum, whereas α for the small fluctuations is large and located in the right tail of the spectrum. Accordingly, the multifractality strength is characterized by the large deflection of the local singularity exponent α from the central orientation $\alpha(0)$. When α is almost constant, the signal is mono-fractal, while α variations indicate a multi-scaling process (Ihlen and Vereijken 2013; Cruz and Sampaio 2020).

The range α illustrates the variety of singularity exponents, resembling the dynamics of the system, and the value of $\Delta f(\alpha)$ represents the probability of an identified α . The singularity spectrum may be categorized in three, regarding the shape. Accordingly, a singularity spectrum with a left long tail, right long tail, and symmetric spectrums can be identified. This subdivision comes from the range of a singularity spectrum which includes a left limb (L) and a right limb (R), representing the dynamics of the highest and lowest fluctuations, respectively. When the mean values of $\Delta f(\alpha) > 0$, the minimum fluctuation rate in the time series happens with a higher probability than the maximal fluctuation rate, and the signal structure is not sensitive to local fluctuations with a large magnitude. Likewise, when the mean values of $\Delta f(\alpha) < 0$, then the maximal fluctuation rate occurs with a higher probability comparing the minimal rate and the signal structure is not sensitive to small magnitude local fluctuations (Cruz and Sampaio 2020). It has to be mentioned that the MATLAB software was used for multifractal analysis, and MATLAB, Microsoft Office, and DEEPSOIL softwares were employed to generate the graphs.

Results and discussion

The analysis was performed in two phases. In the first phase, shear strain percentage and 5% damped spectral acceleration diagrams were plotted and interpreted. In the second phase, the dynamic properties of the motions’ significant duration were estimated, and the possible relationship between the nonlinear dynamic properties of motions’ significant duration and resonance phenomena in soil and soil failure was investigated.

Phase 1 results

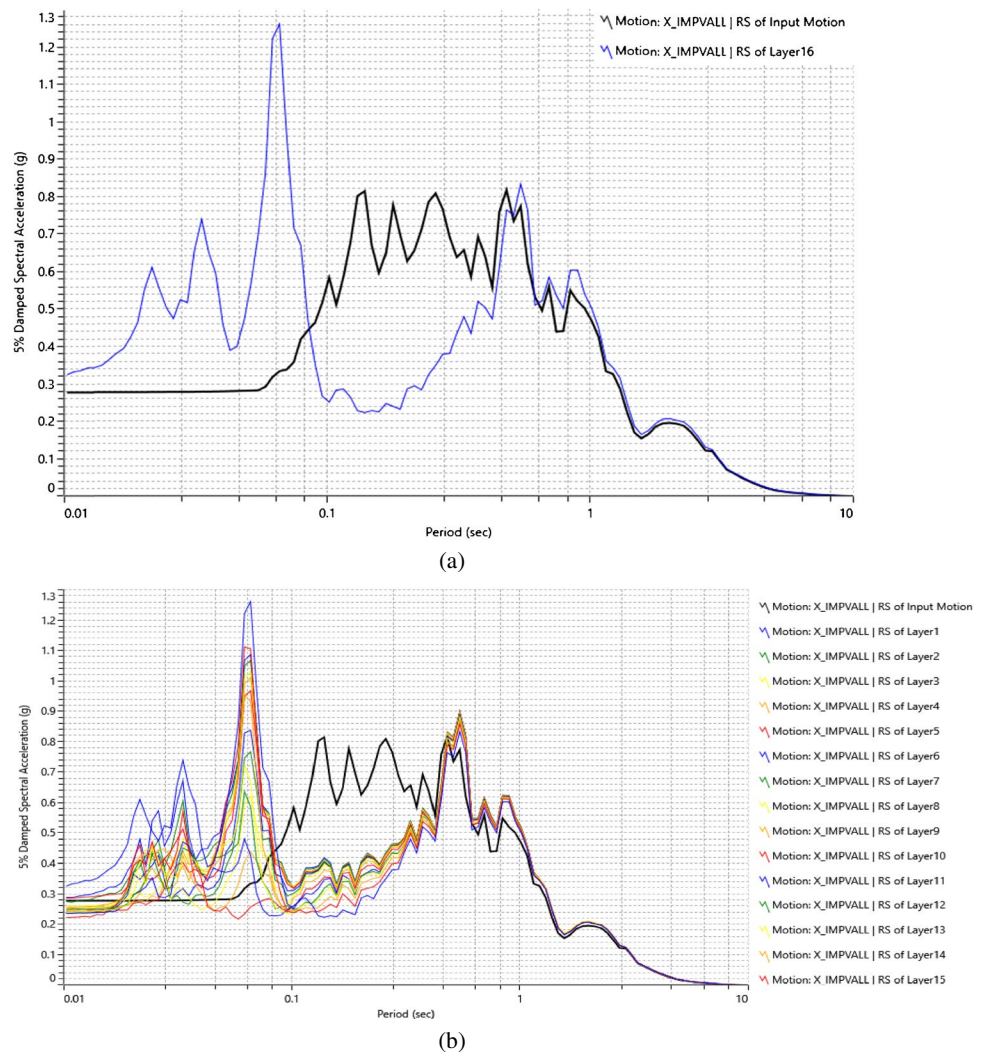
After generating the soil profile described in the “Materials and methods” section, ten ground motions were applied to the produced soil profile, and the shear strain percentage and 5% damped spectral acceleration diagrams were generated. An examination of the 5% damped spectral acceleration graphs revealed that all ground motions, except those in El Alamo and Trinidad, produced resonance in the soil. In cases where ground motions resonated, they did so within a period of less than 0.1 s and from 1 to 8 s. However, in the period of less than 0.1 seconds, the rate of intensification was considerable, and in the period from 1 to 8 seconds, it was negligible. A striking example of resonance in soil was produced in Imperial Valley (II) (Fig. 2).

Figure 2a clarifies that between the period of 0.01 and 0.08 s, considerable resonance was produced by Imperial Valley (II) ground motion (layer 16’s response spectra (RS) curve (blue line) exceeded response spectra of input motion (black line)). This demonstrates that during this period, the

soil profile is considerably prone to resonance and buildings that have a natural frequency from 0.01 to 0.08 s will be severely damaged. In the period between 0.5 and 1 s, intensification (resonance in soil) was detected, although it was slight.

Figure 2b illustrates that the generated soil profile experienced resonance in all layers. The highest resonance occurred at the period of 0.06 s, which was equal to 1.26 g. In cases where resonance was produced in the soil profile, layers 15 and 16 were the most sensitive layers and experienced the highest resonance. Layers close to the surface witnessed insignificant resonance. However, for some ground motions, the resonance recorded in layers 15 and 16 was insignificant, while it was noticeable in others. According to $F = \frac{1}{T}$ (F = frequency, T = period), the earthquake frequency is high during low periods and vice versa. Figure 2b shows that the resonance occurred in the first part of the diagram, verifying that the soil resonated at high frequencies. Hence, although high-rise buildings will be damaged, short-rise structures will be safe. In the second part of the diagram

Fig. 2 5% damped spectral acceleration versus period graph concerning Imperial Valley (II) input ground motion and the sixteen layers of generated soil profile



(Fig. 2b), there was an insignificant resonance, illustrating that the soil profile has low resonance at low frequencies and high periods, meaning that short-rise buildings are safe.

During the period from 0.08 to 0.4 s, the RS lines of the different layers (the colored lines in Fig. 2b) were significantly lower than the RS line of the input motion (the black line in Fig. 2b). This indicated that the soil damped the earthquake motions well during this period and prevented resonance in the soil profile. The most significant resonances occurred in layers 15 and 16. For this soil sample, the occurrence of earthquakes poses the greatest risk to underground structures (such as basements, underground tunnels, and underground parking lots).

The shear strain percentage graphs (Fig. 3) indicate that few ground motions brought about the soil failure phenomenon (Cape Mendocino, Kobe, Loma Prieta, and Gazli). Also, an examination of shear strain percentage and 5% damped spectral acceleration graphs did not confirm a significant relationship between the intensity of resonance in the soil and soil rupture (soil failure phenomenon). As a case in point, consider Imperial Valley (II). Even though Imperial Valley (II) produced the most significant resonance in soil,

Loma Prieta's ground motion led to the most soil rupture in the generated soil profile. All ground motions that caused the soil failure produced resonance in the soil; however, the opposite effect was not valid. The Loma Prieta shear strain percentage graph is presented in Fig. 3 as an illustration.

Between 11 and 12 s, the percentage of shear strain exceeded 1% (touched 8%), indicating soil failure (experienced in layer 16). All soil failures occurred in layers 15 and 16, with layer 16 experiencing more extensive ruptures than layer 15.

Phase 2 results

In this phase, the nonlinear dynamic properties of ground motions were investigated. The significant duration was calculated before dynamic analysis. If the entire earthquake signal is analyzed, there is a high probability that the multifractal or mono-fractal behavior of the signal will not be detected. For this reason, only the significant duration part of the earthquake signal was analyzed. An example is the significant duration graph of Loma Prieta motion (Fig. 4).

Fig. 3 The Loma Prieta's shear strain percentage graph

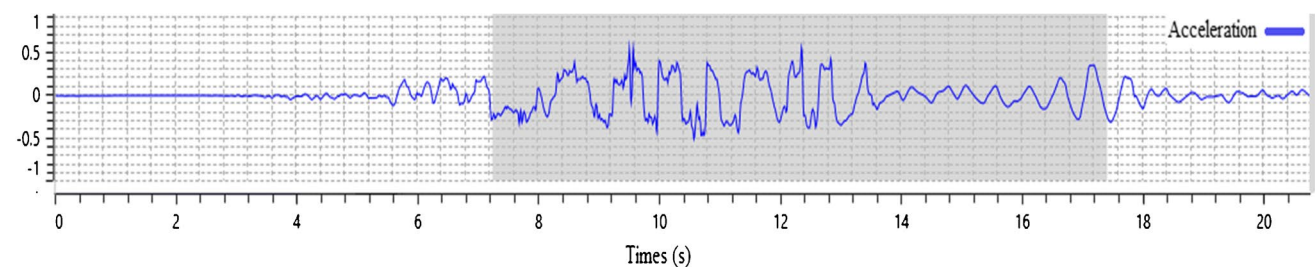
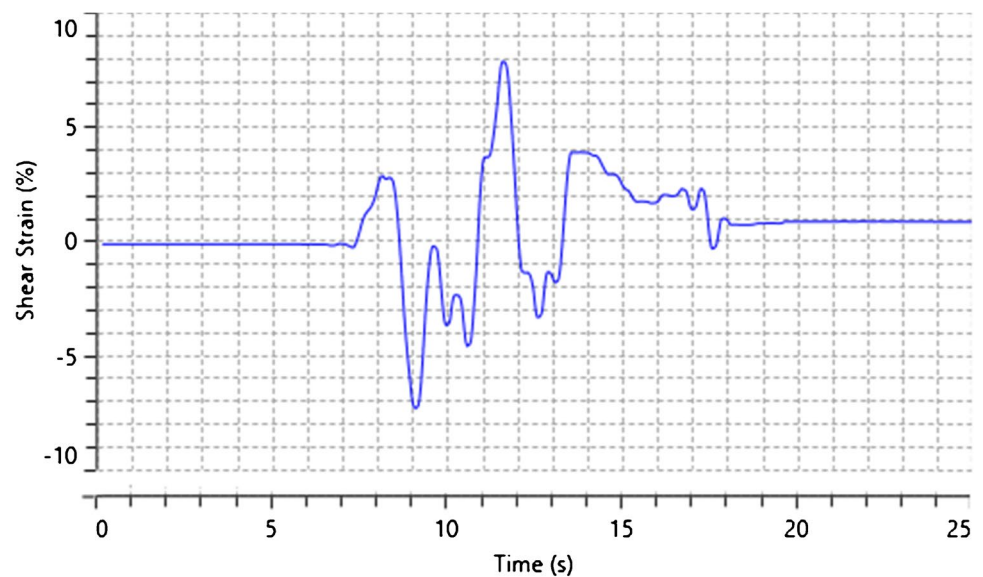


Fig. 4 The significant duration of Loma Prieta motion marked in gray on the graphs

As shown in Fig. 4, the significant duration of Loma Prieta motion was from 6.56 to 14.375 s.

Figure 5 shows the multifractal singularity spectrum diagrams.

Figure 5 shows that the singularity spectrum curves of the Cape Mendocino, Trinidad, Kobe, and El Alamo motions were of the right-tailed type. This indicates that the probability of small fluctuations (minute accelerations) in the acceleration time series of these motions was higher than large fluctuations—likewise, their signals were not sensitive to large local fluctuations. Smart (Taiwan), Loma Prieta, and Spitak (Armenia) motions showed left-tail singularity

spectrum curves, designating more large fluctuations (acceleration magnitude) and less sensitivity to small fluctuations in their earthquake signals. The singularity spectrum curves of Gazli, Imperial Valley (II), and Borah Peake motions were symmetric, which indicates the equal extent of low and high fluctuations in their motion signals. Regulations 2800 (2014) suggest that accelerations in earthquake waves with small magnitudes, compared to those with large magnitudes, intensify the ground’s response. Therefore, they produce minute strains in the soil structure, leading to an escalation in the resonance probability in the soil. Accordingly, the resonances caused by Imperial Valley (II), Gazli, Borah Peake, Kobe, and Cape Mendocino motions were justifiable and expected.

The mean generalized Holder exponent $\alpha(0)$ values of Cape Mendocino, Borah Peake, Imperial Valley (II), and Gazli motions were less than 0.5, indicating long memory with anti-correlated conduct. Regarding Smart (Taiwan), Loma Prieta, El Alamo, Kobe, Trinidad, and Spitak (Armenia) motions, the mean generalized Holder exponent $\alpha(0)$ values were higher than 0.5, demonstrating the correlated attitude of ground motions (earthquake signals). The results reveal that all the ground motions with a mean generalized Holder exponent $\alpha(0)$ greater than 0.5 triggered resonance in the soil. The results also suggest that the anti-correlated behavior of fluctuations in earthquake waves (ground motions) enhanced the resonance likelihood in soil.

By computing $\Delta\alpha$ values (Figs. 5 and 6) diagrams, the multifractal singularity spectrum width was measured and interpreted. The results show that the Kobe motion possessed the highest $\Delta\alpha$ value, meaning that this motion had the most multifractal behavior, whereas the Spitak motion manifested the most inconsiderable multifractal behavior.

The multifractal singularity spectrum width revealed that all ground motions held mono-scale structures, except for

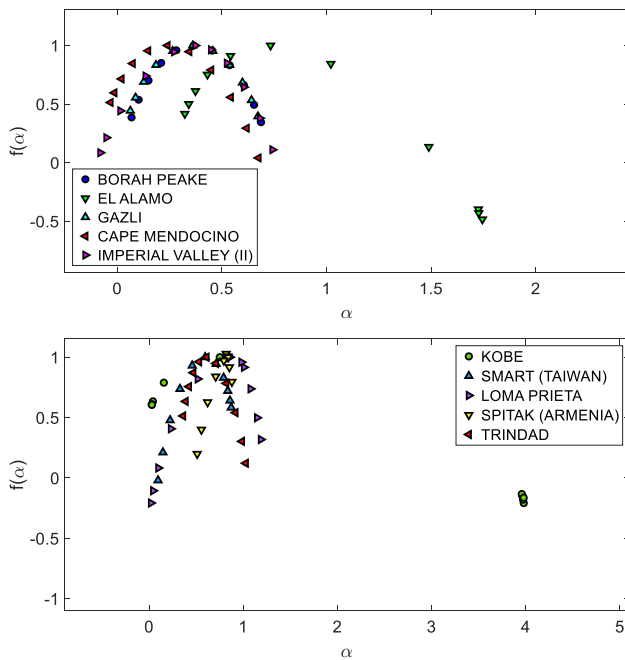
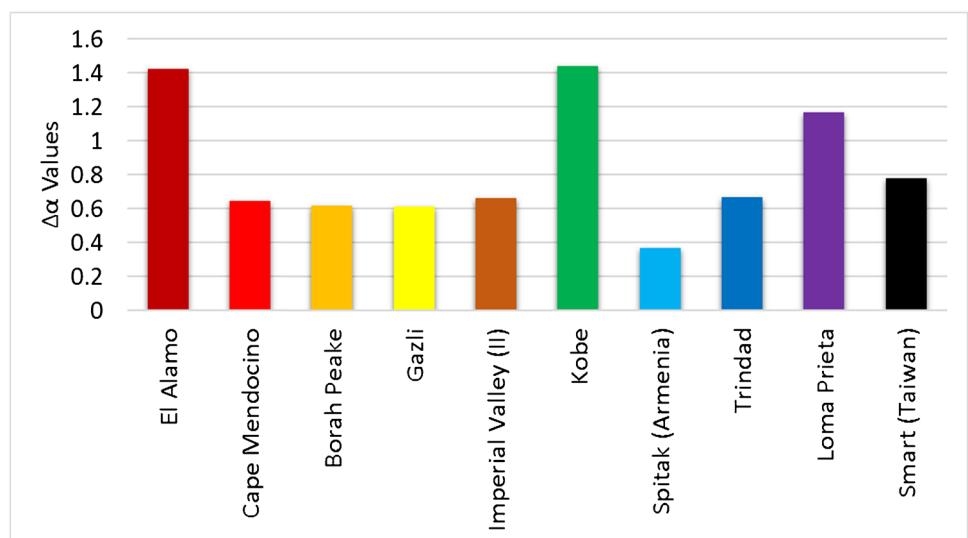


Fig. 5 The multifractal singularity spectrum of ground motions

Fig. 6 The $\Delta\alpha$ values concerning the ten study ground motions



those of El Alamo, Kobe, and Loma Prieta, as these ground motions were multifractal. The results indicated that ground motions with a single-scale structure considerably increased the likelihood of resonance in the soil.

An examination of the results of phases 1 and 2 reveal that ground motions with either mono-scale or multi-scale and with symmetrical- or right-tail singularity spectrum augment the likelihood of resonance in soil. Even though dynamic properties and repetitive patterns in ground motions (earthquakes) had no effect on resonance frequency and period, they amplified the likelihood of resonance in soil. Since considerable resonances in soil bring about soil structure failure, one can conclude that ground motions escalate the probability of soil failure if ground motions have (1) right-tail or symmetrical singularity spectrum curves and (2) mono-scale structures.

The earthquake signals (ground motions) applied for the analysis in phases one and two were in the X direction. Comparable computations and analyses were performed for the earthquake signals in the Y and Z directions presented similar results. In other words, the dynamic properties of earthquake acceleration in all three axes (X, Y, and Z) had similar effects on resonance in the soil.

Studies on soil resonance conducted by the Roads, Housing, and Urban Development Research Center suggested that in addition to the soil structural properties (materials and thickness), the frequency and duration of the arrival of earthquake waves into the soil are significant. The present study broadened the general understanding of the impacts of the nonlinear dynamic properties of earthquake signals (ground motions, earthquake waves) on resonance in soil. The present study showed that the dynamic properties of ground motions play a role in resonance in soil.

To the best of the authors' knowledge, no studies to date have examined the relationship between the nonlinear dynamic characteristics of earthquake waves and resonance in soil and soil failure.

Conclusion

This study incorporated the influence of nonlinear dynamic properties of earthquake acceleration (ground motions) on resonance in soil. The study is relevant due to the importance of the resonance in the soil for structural design. A soil profile was generated, and the effects of nonlinear dynamic properties of ground motions on soil resonance were investigated. The results indicated that all earthquakes, except those in El Alamo and Trinidad, produced resonance in the generated soil profile. Also, the critical periods during which the ground motions resonated were less than 0.1 s and from 1 to 8 s. Moreover, layers close to the bedrock (15 and 16) experienced the highest resonance, while layers close to the surface experienced

inconsiderable resonance. If the earthquake signals (ground motions) meet at least one of the following conditions, the resonance probability in the soil increases significantly: (1) The earthquake signal has a right-tail or symmetrical multifractal singularity spectrum curve, (2) the earthquake signal holds a mono-scale structure, or (3) the earthquake signal exhibits long memory with anti-correlated behavior.

An analysis of the effect of earthquake acceleration in the Y and Z directions on soil resonance provided similar results to that in the X direction. Even though dynamic properties and repetitive patterns in ground motions (earthquakes) had no effect on resonance frequency and period, they amplified the likelihood of resonance in soil. This study revealed the influence of dynamic properties of earth movements on resonance in soil. Specifically, the results suggest that, in the case of structural design, when assessing the risk of resonance in the soil, only ground motions that include at least one of the above conditions should be considered. In other words, ground motions with the mentioned characteristics increase the possibility of creating a significant resonance in the soil, bringing about serious damage to structures. This study proposed a new perspective on resonance in soil, and future studies can examine the effect of intrinsic characteristics of ground motions on resonance in soil by considering statistical parameters that were not addressed in this study.

Author contribution Conceptualization: Farhang Rahmani. Methodology: Farhang and Hanif Rahmani. Formal analysis and investigation: Farhang and Hanif Rahmani. Writing, original draft preparation; writing, review and editing; supervision: Farhang Rahmani.

Data Availability Some or all data and models that support the findings of this study are available from the corresponding author upon reasonable request. The corresponding author is ready to share data with other researchers who send their request to this email address: farhang.rahmani@miau.ac.ir.

Code availability Codes that support the findings of this study are available from the corresponding author upon reasonable request. The corresponding author is ready to share data with other researchers who send their request to this email address: farhang.rahmani@miau.ac.ir.

Declarations

Ethics approval Not applicable.

Consent to participate Not applicable.

Consent for publication Not applicable.

Conflict of interest The authors declare no competing interests.

References

Adarsh S, Dharan DS, Nandhu AR et al (2020) Multifractal description of streamflow and suspended sediment concentration data

- from Indian river basins. *Acta Geophys* 68:519–535. <https://doi.org/10.1007/s11600-020-00407-2>
- Alam Z, Sun L, Zhang C, Su Z, Samali B (2021) Experimental and numerical investigation on the complex behaviour of the localised seismic response in a multi-storey plan-asymmetric structure. *Struct Infrastruct Eng* 17(1):86–102. <https://doi.org/10.1080/15732479.2020.1730914>
- Alimohammadi H, Yaghin ML (2019) Study on the effect of the concentric brace and lightweight shear steel wall on seismic behavior of lightweight steel structures. *Int Res J Eng Technol* 203:0–3
- Alimohammadi H, Esfahani MD, Yaghin ML (2019a) Effects of openings on the seismic behavior and performance level of concrete shear walls. *Int J Appl Sci* 6(10):34–39. <https://doi.org/10.31873/IJEAS.6.10.10>
- Alimohammadi H, Hesaminejad A, Yaghin ML (2019b) Effects of different parameters on inelastic buckling behavior of composite concrete-filled steel tubes. *Int Res J Eng Technol* 6(12):603–609. <https://doi.org/10.31224/osf.io/wqgj8>
- Alimohammadi H, Dastjerdi K, Yaghin M (2020) The study of progressive collapse in dual systems. *Civ Environ Eng* 16(1):79–85. <https://doi.org/10.2478/cee-2020-0009>
- Cruz IF, Sampaio J (2020) Multifractal analysis of movement behavior in association football. *Symmetry* 12:1287. <https://doi.org/10.3390/sym12081287>
- Diaz-Fanas G, Garini E, Ktenidou OJ, Gazetas G, Vaxevanis T, Lan YJ, Heintz J, Ma X, Korre E, Valles-Mattox R, Stavridis A (2020) ATC Mw7. 1 Puebla–Morelos earthquake reconnaissance observations: Seismological, geotechnical, ground motions, site effects, and GIS mapping. *Earthquake Spectra* 36(2_suppl):5–30. <https://doi.org/10.1177/8755293020964828>
- Douglas J, Aochi H, Suhadolc P, Costa G (2007) The importance of crustal structure in explaining the observed uncertainties in ground motion estimation. *Bull Earthq Eng* 5(1):17–26. <https://doi.org/10.1007/s10518-006-9017-y>
- Gallipoli MR, Calamita G, Tragni N, Pisapia D, Lupo M, Mucciarelli M, Stabile TA, Perrone A, Amato L, IZZI F, La Scaleia G (2020) Evaluation of soil-building resonance effect in the urban area of the city of Matera (Italy). *Eng Geol* 272:105645. <https://doi.org/10.1016/j.enggeo.2020.105645>
- Garcia-Suarez J, Asimaki D (2020) On the fundamental resonant mode of inhomogeneous soil deposits. *Soil Dyn Earthq* 135:106190. <https://doi.org/10.1016/j.soildyn.2020.106190>
- Gosar A, Rošer J, Šket Motnikar B et al (2010) Microtremor study of site effects and soil-structure resonance in the city of Ljubljana (central Slovenia). *Bull Earthq Eng* 8:571–592. <https://doi.org/10.1007/s10518-009-9113-x>
- Groholski D, Hashash Y, Kim B, Musgrove M, Harmon J, Stewart J (2016) Simplified model for small-strain nonlinearity and strength in 1D seismic site response analysis. *J Geotech Geoenviron Eng* 142(9):04016042. [https://doi.org/10.1061/\(ASCE\)GT.1943-5606.0001496](https://doi.org/10.1061/(ASCE)GT.1943-5606.0001496)
- Guangyin D, Changhui G, Songyu L et al (2021) Resonance vibration approach in soil densification: laboratory experiences and numerical simulation. *Earthq Eng Vib* 20:317–328. <https://doi.org/10.1007/s11803-021-2022-y>
- Halliday D, Resnick R, Walker J (2005) *Fundamentals of Physics, part 2* (7th ed.) edn. John Wiley & Sons Ltd, Hoboken ISBN 978-0-471-71716-4
- Ihlen EA, Vereijken B (2013) Multifractal formalisms of human behavior. *Hum Mov Sci* 32(4):633–651. <https://doi.org/10.1016/j.humov.2013.01.008>
- Kaiser PK, McCreath DR, Tannant DD (1996) Canadian rockburst support handbook. Canadian Rockburst Research Program, Camiro
- Kantelhardt JW, Zschiegner SA, Koscielny-Bunde E, Bunde A, Havlin S, Stanley HE (2002) Multifractal detrended fluctuation analysis of nonstationary time series. *Physica A* 316:87. [https://doi.org/10.1016/S0378-4371\(02\)01383-3](https://doi.org/10.1016/S0378-4371(02)01383-3)
- Kaurkin MD, Romanov VV, Andreev DO (2021) Assessment of the effect of resonance properties of soils during seismic microzonation. In: Svalova V (ed) *Heat-Mass Transfer and Geodynamics of the Lithosphere. Innovation and Discovery in Russian Science and Engineering*. Springer, Cham. https://doi.org/10.1007/978-3-030-63571-8_27
- Lindfield G, Penny J (2019) Chapter 5 - solution of differential equations. In: *Numerical Methods*, 4th edn. Academic Press, London, pp 239–299. <https://doi.org/10.1016/B978-0-12-812256-3.00014-2>
- Ma J, Dong L, Zhao G, Li X (2018) Qualitative method and case study for ground vibration of tunnels induced by fault-slip in underground mine. *Rock Mech Rock Eng* 52:1887–1901. <https://doi.org/10.1007/s00603-018-1631-x>
- Ma J, Dong L, Zhao G, Li X (2019) Ground motions induced by mining seismic events with different focal mechanisms. *Int J Rock Mech Min* 116:99–110. <https://doi.org/10.1016/j.ijrmms.2019.03.009>
- Mandelbrot BB (1989) Multifractal measures, especially for the geophysicist. In: *InFractals in geophysics*. Birkhäuser, Basel, pp 5–42. https://doi.org/10.1007/978-3-0348-6389-6_2
- Mase LZ, Likitlersuang S, Tobita T (2021) Ground motion parameters and resonance effect during strong earthquake in Northern Thailand. *Geotech Geol Eng* 39:2207–2219. <https://doi.org/10.1007/s10706-020-01619-5>
- Miloš LR, Hačiegan C, Miloš MC, Barna FM, Božoc C (2020) Multifractal detrended fluctuation analysis (MF-DFA) of stock market indexes. *Empirical Evidence from Seven Central and Eastern European Markets*. *Sustainability* 12(2):535. <https://doi.org/10.3390/su12020535>
- Moschetti MP, Hatzell SH (2021) Spectral Inversion for seismic site response in Central Oklahoma: low-frequency resonances from the great unconformity. *Seismol Soc Am Bull* 111(1):87–100. <https://doi.org/10.1785/0120200220>
- Munro MA, Ord A, Hobbs BE (2018) Spatial organization of gold and alteration mineralogy in hydrothermal systems: wavelet analysis of drillcore from Sunrise Dam Gold Mine, Western Australia. *Geol Soc Lond Spec Publ* 453(1):165. <https://doi.org/10.1144/SP453.10>
- Ottoneilli D, Manzini CF, Marano C, Cordasco EA, Cattari S (2021) A comparative study on a complex URM building: part I—sensitivity of the seismic response to different modelling options in the equivalent frame models. *Bull Earthq Eng* 20:2115–2158, 1–44. <https://doi.org/10.1007/s10518-021-01128-7>
- Pavel F, Vacareanu R, Pitilakis K, Anastasiadis A (2020) Investigation on site-specific seismic response analysis for Bucharest (Romania). *Bull Earthq Eng* 18:1933–1953. <https://doi.org/10.1007/s10518-020-00789-0>
- Phillips C, Hashash Y (2009) Damping formulation for non-linear 1D site response analyses. *Soil Dyn Earthq Eng* 29:1143–1158
- Rahmani F, Fattahi MH (2021a) A multifractal cross-correlation investigation into sensitivity and dependence of meteorological and hydrological droughts on precipitation and temperature. *Nat Hazards* 109:2197–2219. <https://doi.org/10.1007/s11069-021-04916-1>
- Rahmani F, Fattahi MH (2021b) Nonlinear dynamic analysis of the fault activities induced by groundwater level variations. *Groundw Sustain Dev* 14:100629. <https://doi.org/10.1016/j.gsd.2021.100629>
- Regulations 2008 (2014) *Earthquake design regulations in Iran (Regulations 2800)*, 4th Edition. Roads, Housing and Urban Development Research Center. <http://www.nbri.ir/%D9%85%D8%A8%D8%A7%D8%AD%D8%AB-%D9%85%D9%82%D8%B1%D8%B1%D8%A7%D8%AA-%D9%85%D9%84%DB%8C-%D8%B3%D8%A7%D8%AE%D8%AA%D9%85%D8%A7%D9%86>. Accessed 25 Mar 2021

- Sgattoni G, Castellaro S (2020) Detecting 1-D and 2-D ground resonances with a single-station approach. *Geophys J Int* 223(1):471–487. <https://doi.org/10.1093/gji/ggaa325>
- Trevisani S, Pettenati F, Paudyal S, Sandron D (2021) Mapping long-period soil resonances in the Kathmandu basin using micro-tremors. *Environ Earth Sci* 80:265. <https://doi.org/10.1007/s12665-021-09532-7>
- Xie W, Sun L, Lou M (2020) Shaking table test verification of traveling wave resonance in seismic response of pile-soil-cable-stayed bridge under non-uniform sine wave excitation. *Soil Dyn Earthq* 134:106151. <https://doi.org/10.1016/j.soildyn.2020.106151>
- Zhang X, Liu H, Zhao Y, Zhang X (2019) Multifractal de-trended fluctuation analysis on air traffic flow time series: a single airport case. *Physica A* 531:121790. <https://doi.org/10.1016/j.physa.2019.121790>
- Zheng J, He H, Alimohammadi H (2021) Three-dimensional Wadell roundness for particle angularity characterization of granular soils. *Acta Geotech* 16:133–149. <https://doi.org/10.1007/s11440-020-01004-9>